Dissociation and Keto-Enol Tautomerism of Phloroglucinol and Its Anions in Aqueous Solution

Martin Lohrie and Wilhelm Knoche*

Contribution from the Fakultät für Chemie, Universität Bielefeld, Universitätsstrasse 25, D-4800 Bielefeld 1, FRG. *Received July 28, 1992*

Abstract: Dissociation and keto–enol tautomerism of phloroglucinol and its anions lead to the formation of ten species with different degrees of dissociation and conjugation. The equilibria between these species have been determined by applying kinetic techniques. The transition from the phenolic to the ketonic forms is connected with the protonation of the aromatic ring and leads to the formation of σ-complexes. The rate constants for these reactions have been determined and compared with data of other σ-complex formations.

Introduction

As early as 1886, A. Baeyer observed that phloroglucinol (1,3,5-trihydroxybenzene) forms a trioxime with hydroxylamine.[1] This reaction is typical for ketones, and therefore he concluded that phloroglucinol may exist in the triketo form **10** (the bold numbers refer to Scheme II, see below). Alkylation leads either to O- or to C-substituted products, indicating an aromatic or a carbonylic structure of phloroglucinol, respectively, depending upon the specific conditions of the reaction.[2] This ambivalent behavior induced a number of investigations examining the keto–enol equilibria of the neutral phloroglucinol and of its mono- and di-deprotonated anions.[3] The neutral molecule exists nearly exclusively in the aromatic form **1**, whereas the conjugated ketonic form **5** prevails for the dianion. This has been shown in particular by the work of Highet[4] and of Scheibe and Köhler,[5] evaluating ^{1}H-NMR data and comparing UV/vis-spectra of phloroglucinol with spectra of the dianion of filicinic acid, respectively. The aromatic form has been proposed for the monoanion,[4] although this result is less reliable, since the monoanion predominates at no pH (the pK_1 and pK_2 values of phloroglucinol are similar). Thermodynamic data for the keto–enol equilibrium and systematic investigations concerning the kinetics of the conversion have not been published so far, so that the present knowledge of the keto–enol tautomerism of phloroglucinol is unsatisfactory.[6]

Furthermore, the keto–enol conversion is linked to the formation of σ-complexes, which are of great importance as intermediates in electrophilic aromatic substitutions. In aqueous solution at pH > 0, stable σ-complexes are obtained by the protonation of azulenes[7] and triaminobenzenes.[8] For phloroglucinol, Kresge[9] and Schubert and Quacchia[10] observed the formation of a σ-complex with structure A (Scheme II), investigating the protonation at the aromatic ring in superacidic media (pH < 0). Further σ-complexes should be formed by ring-protonation of the three differently deprotonated aromatic anions of phloroglucinol. These σ-complexes are expected to be strongly stabilized by the negatively charged oxygen substituents, so that they should be stable in aqueous solutions at pH > 0. As an example, Scheme I shows three mesomeric structures of the nonaromatic dianion, where y is the structure of a typical σ-complex and its stabilization is indicated by the carbonyl forms x and z; i.e. the σ-complex and ketones are mesomeric forms of the same compound. (In Scheme II structure x is written, as is usually done in the literature.)

Scheme I

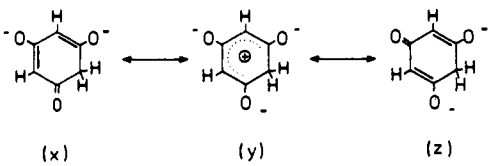

(x) (y) (z)

Experimental Section

Most kinetic experiments were performed using a UV/vis stopped-flow apparatus with a dead-time of about 3 ms, where equal volumes of solutions of phloroglucinol and of buffer are mixed. Spectra of the intermediates were recorded using a diode-array spectrophotometer HP 8452A equipped with a stopped-flow mixing unit. Under equilibrium conditions, spectra were recorded with a spectrophotometer Kontron Uvicon 860. In those three apparatuses, the length of the cuvettes is 1 cm. Temperature-jump and pressure-jump relaxation techniques were used for supplementary measurements.

All chemicals are commercially available (grade p.a.) and were used without further purification. For the solutions, tridistilled water was used, which was carefully degassed in order to remove CO_2. The pH of the solutions was adjusted by the addition of HCl (pH < 4.0), NaOH (pH > 10.4), and the buffer systems CH_3COONa/HCl (4.0 < pH < 5.4), Na_2HPO_4/HCl (6.0 < pH < 7.9), Tris/HCl (7.5 < pH < 9.1), NH_4Cl/NaOH (8.6 < pH < 9.9), and Na_2CO_3/HCl (9.2 < pH < 10.4). The pH values were calculated from the concentrations and the dissociation constants of the buffers, and they were measured using a glass electrode. Calculated and experimentally obtained values agreed within ±0.03 unit.

The kinetic measurements were performed in buffered solutions, i.e. $[H^+]$ = constant. Therefore the reactions proceed under pseudo-first-order conditions, and for all experiments the time dependence of the absorbance fits to eq 1 or 2. These equations describe one or two

$$A(t) = (A_0 - A_e)\exp(-t/\tau_S) + A_e \quad (1)$$

$$A(t) = (A_0 - A_1)\exp(-t/\tau_F) + (A_1 - A_e)\exp(-t/\tau_S) + A_e \quad (2)$$

superimposed relaxation effects with relaxation times τ_i and amplitudes (A_i-A_j). F and S indicate the fast and slow relaxation effect, respectively.

The pH dependence of the absorbance A_0, A_1, and A_e was evaluated according to eqs 3 and 4 corresponding to a one- and a two-photon process, respectively. In both equations activity corrections are considered dependent upon the charge of the ions involved. Π_1 and Π_2 are the products of the activity coefficients, which are calculated by Davies' equation,[11] and they are indicated by i = I, II, and III for monovalent, divalent, and trivalent ions, respectively. Inert salt was not added to the solutions, and the ionic strength was calculated from the concentrations

$$\frac{A}{d} = \frac{\epsilon_a K\Pi + \epsilon_b c_H}{K\Pi + c_H} c_0 \quad (3)$$

$$\frac{A}{d} = \frac{\epsilon_a K_1 K_2 \Pi_1 \Pi_2 + \epsilon_b K_2 \Pi_2 c_H + \epsilon_c c_H^2}{K_1 K_2 \Pi_1 \Pi_2 + K_2 \Pi_2 c_H + c_H^2} c_0 \quad (4)$$

(1) Baeyer, A. *Ber. Dtsch. Chem. Ges.* **1886**, *19*, 159–163.
(2) Herzig, J.; Erthal, B. *Monatsh. Chem.* **1910**, *31*, 827.
(3) Ershov, V. V.; Nikiforov, G. A. *Russ. Chem. Rev.* **1966**, *35*, 817–833.
(4) Highet, R. J.; Batterham, T. J. *J. Org. Chem.* **1964**, *29*, 475–476.
(5) Köhler, H.; Scheibe, G. *Z. Anorg. Allg. Chem.* **1956**, *285*, 221–235.
(6) Highet, R. J.; Ekhato, I. V. *J. Org. Chem.* **1988**, *53*, 2843–2844.
(7) Challis, B. C.; Long, F. A. *J. Am. Chem. Soc.* **1965**, *87*, 1196–1202.
(8) Knoche, W.; Schoeller, W. W.; Schomäcker, R.; Vogel, S. *J. Am. Chem. Soc.* **1988**, *110*, 7484–7491.
(9) Kresge, A. J.; Chiang, Y.; Hakka, L. E. *J. Am. Chem. Soc.* **1971**, *93*, 6167–6173.
(10) Schubert, W. M.; Quacchia, R. H. *J. Am. Chem. Soc.* **1963**, *85*, 1278–1284, 1284–1289.
(11) Davies, C. W. J. *Ion Association*; Butterworth: London, 1962.

0002-7863/93/1515-919$04.00/0

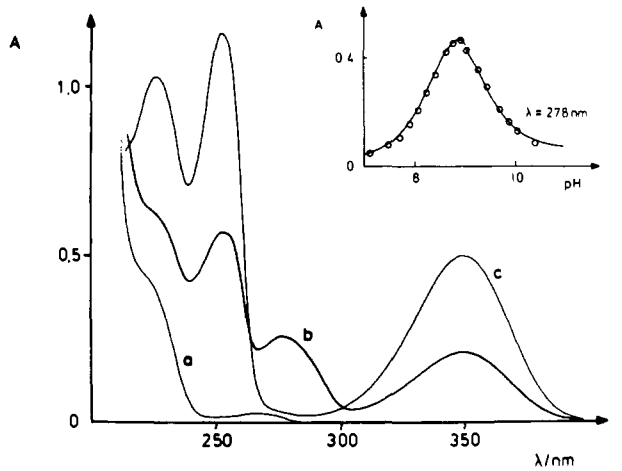

Figure 1. Spectra of 5×10^{-5} M solutions of phloroglucinol at equilibrium: a, pH = 5; b, pH = 9; c, pH = 12. Inset: Spectrophotometric titration of 1×10^{-4} M solutions of phloroglucinol. The curves are calculated according to eq 4.

of acid, base, and buffer. All results reported refer to 20 °C and 1 bar.

Results

The spectra in Figure 1 indicate the existence of three differently protonated species of phloroglucinol. Below pH = 7 it does not dissociate, and at pH > 11 it is twice deprotonated. At pH = 9 the absorbance maximum at 278 nm has to be attributed to the mono-deprotonated anion, but the undissociated molecule and the dianion of phloroglucinol exist simultaneously; i.e., at no pH value does the mono-deprotonated form predominate strongly. This can be seen in the titration curve (inset of Figure 1). At λ = 278 nm the absorbance increases at pH > 7 due to the formation of the monoanion, but before the equilibrium is shifted completely, the absorbance decreases again due to the second deprotonation. The numerical evaluation according to eq 4 yields for the dissociation constants the values $pK_{a1} = 8.8 \pm 0.2$ and $pK_{a2} = 9.0 \pm 0.1$. Activity corrections have been considered in the calculations; i.e., the values refer to ionic strength $I = 0$. At pH > 13 the absorbance changes again, and at pH ≃ 14.5 the spectrum resembles closely that for pH < 7. For this third dissociation step we obtain $pK_{a3} = 14.1 \pm 0.1$ at $I = 1$ mol dm^{-3}. Only those three constants can be determined under equilibrium conditions. Our values are close to $pK_{a1} = 8.5$ and $pK_{a2} = 8.9$ quoted by Abichandani and Jatkar.[12]

Further information is obtained from stopped-flow measurements, which are performed under pseudo-first-order conditions. In the first series of experiments we mix solutions of phloroglucinol at pH = 6 with solutions of buffer or NaOH, in order to reach a pH of 8.5–14. A single relaxation effect is observed, as described by eq 1. By reextrapolating to $t = 0$ (time of mixing), we obtain the absorbance A_0, which differs from the initial absorbance A_i at pH = 6 (taking into account the dilution caused by the mixing procedure), whereas the final absorbance A_e agrees with the value of the titration curve in Figure 1. A_i, A_0, and A_e are defined in Figure 2, which shows A_0 as a function of the pH of the solutions. The data fit to eq 3 with $pK_\alpha = 8.90 \pm 0.05$. The spectrum at $t = 0$ has been recorded using the diode-array spectrophotometer. Over the whole pH range, it indicates the existence of aromatic compounds.

In the next series of experiments, basic solutions of phloroglucinol at pH = 11 are mixed with buffer solutions in order to reach a pH of 3–9.5. Now two superimposed relaxation effects are observed corresponding to eq 2. The two relaxation times differ at least by a factor of 10. The amplitudes have the same sign (see Figure 3) or the opposite sign (see Figure 4), depending on the wavelength of observation. Reextrapolating only the slow relaxation effect to $t = 0$ yields A_1. Analogously by reextrapolating

(12) Abichandani, C. T.; Jatkar, S. K. *J. Indian Inst. Sci.* **1938**, *A21*, 417–418.

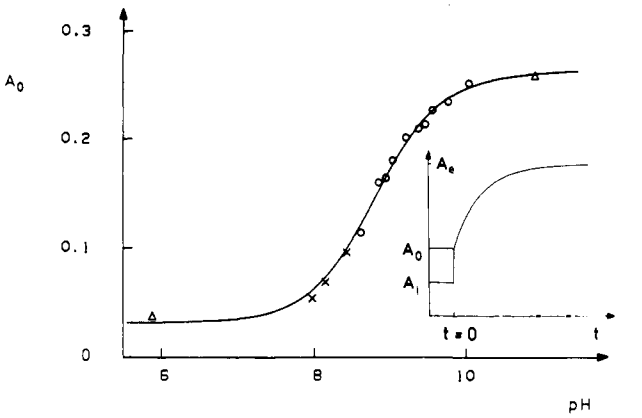

Figure 2. pH dependence of the absorbance A_0 at stopped-flow experiments jumping from neutral to basic solutions: λ = 280 nm; $c_0 = 2 \times 10^{-4}$ mol dm^{-3}; ×, TRIS buffer; ○, ammonium buffer; △, no buffer. The curve is calculated according to eq 3.

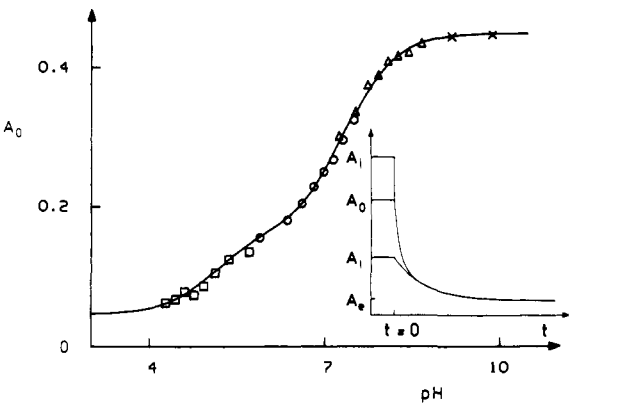

Figure 3. pH dependence of the absorbance A_0 at stopped-flow experiments jumping from pH = 11 to less basic solutions: λ = 350 nm; $c_0 = 5 \times 10^{-5}$ mol dm^{-3}; □, acetate buffer; ○, phosphate buffer; △, TRIS buffer; ×, carbonate buffer. The curve is calculated according to eq 4.

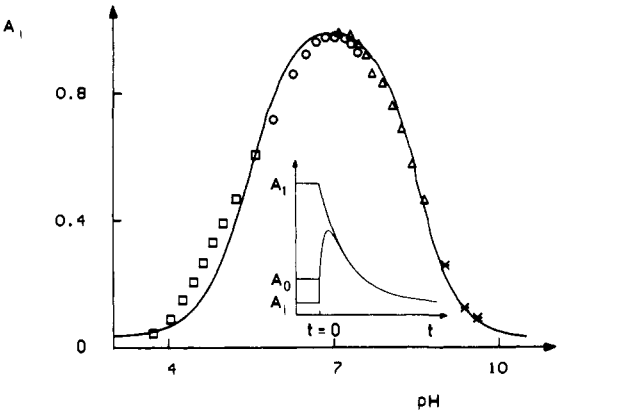

Figure 4. pH dependence of the absorbance A_i at stopped-flow experiments jumping from pH = 11 to less basic solutions: λ = 278 nm; $c_0 = 5 \times 10^{-5}$ mol dm^{-3}; □, acetate buffer; ○, phosphate buffer; △, TRIS buffer; ×, carbonate buffer. The curve is calculated according to eq 4.

both relaxation effects, we obtain A_0. Again A_0 differs from the absorbance A_i at pH = 11, and A_e agrees with the equilibrium values. A_0 and A_i are plotted versus the pH of the solutions in Figures 3 and 4, respectively. Both plots indicate clearly the existence of two protonation steps. By fitting A_0 to eq 4, we obtain $pK_{\beta 1} = 5.14 \pm 0.05$ and $pK_{\beta 2} = 7.43 \pm 0.05$, and from the pH dependence of A_i, we yield $pK_{\gamma 1} = 5.7 \pm 0.1$ and $pK_{\gamma 2} = 8.74 \pm 0.08$. Again the diode-array spectrophotometer allows us to record the spectra of the intermediates, which are displayed at appropriate pH values in Figure 5a for $t = 0$ (corresponding to A_0) and in Figure 5b for a time where the fast reaction has

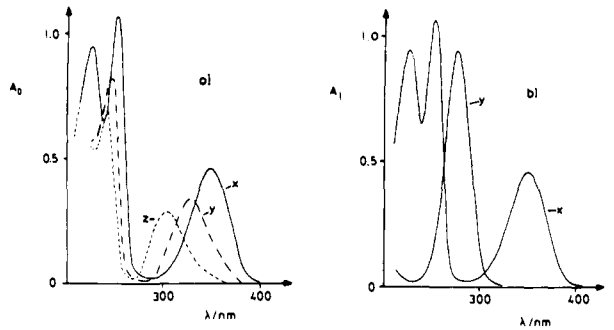

Figure 5. Spectra obtained after mixing a basic solution of phloroglucinol (pH = 11) with acid: $c_0 = 5 \times 10^{-5}$ mol dm^{-3}; ×, spectrum at pH = 11; y, spectrum at pH = 6.2; z, spectrum at pH = 4. (a) Spectra obtained immediately after mixing (A_0). (b) Spectra obtained at a time where the fast relaxation effect has proceeded nearly to equilibrium but where the slow relaxation effect has scarcely started (A_1).

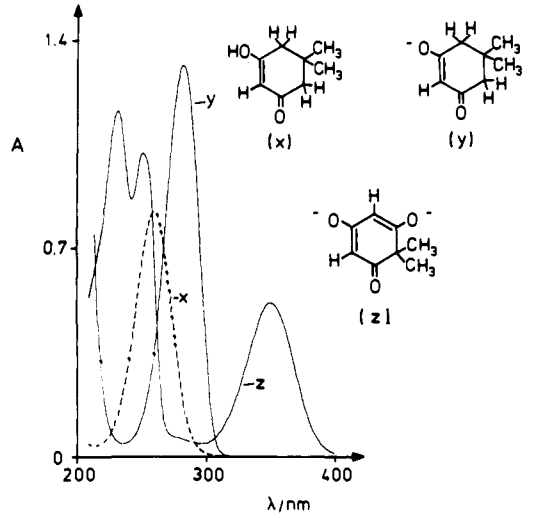

Figure 6. Spectra of dimedone at pH = 3 (×) and at pH = 12 (y) and of filicinic acid at pH = 12 (z).

proceeded nearly to equilibrium but the slow reaction has scarcely started (corresponding to A_1). The spectra of the dienonic dianion of filicinic acid (3,5-dihydroxy-6,6-dimethyl-2,4-cyclohexadien-1-one) and the enonic form of dimedone (5,5-dimethyl-1,3-cyclohexanedione) are recorded and shown in Figure 6 in order to be able to appoint the spectra of the intermediates to certain structures in Scheme II.

The results described so far are not sufficient to evaluate the equilibrium constants involved in the keto–enol equilibria of phloroglucinol. Therefore we performed further kinetic measurements applying the pressure-jump relaxation technique with spectrophotometric detection. Two relaxation effects are observed, but only the faster one is evaluated quantitatively. For constant concentration of phloroglucinol, its amplitude is plotted versus pH in Figure 7. An unsymmetrical bell-shaped curve is obtained with the maximum at pH $\simeq$ 9.

Finally the relaxation times have to be described. The reactions are buffer catalyzed, and therefore the measurements are performed at different buffer concentrations.[13] The reciprocal relaxation times are extrapolated to zero buffer concentration, and these extrapolated values are plotted versus the pH of the solutions in Figure 8. It should be emphasized that, in the pH range where different techniques can be applied, the same values of the relaxation times are obtained from pressure-jump measurements and from both kinds of stopped-flow experiments (pH increase and pH decrease at the mixing). A few measurements are performed using the temperature-jump technique at pH $\simeq$ 14, where in stopped-flow experiments the relatively fast relaxation effect

(13) Lohrie, M. Thesis, Universität Bielefeld, 1991.

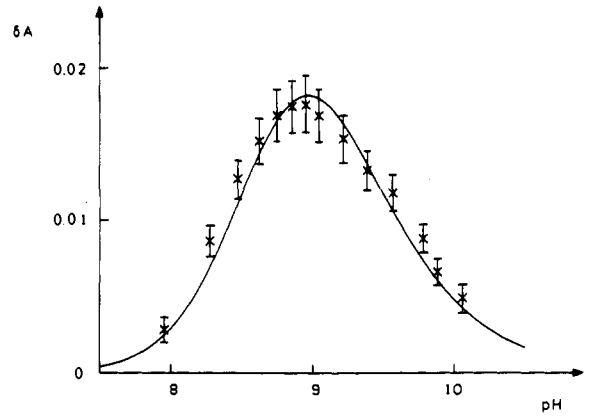

Figure 7. Pressure-jump relaxation amplitudes versus pH for solutions of phloroglucinol in ammonium buffer: λ = 350 nm; $c_0 = 10^{-4}$ mol dm^{-3}; δ_p = 100 bar. The curve is calculated according to eq 17.

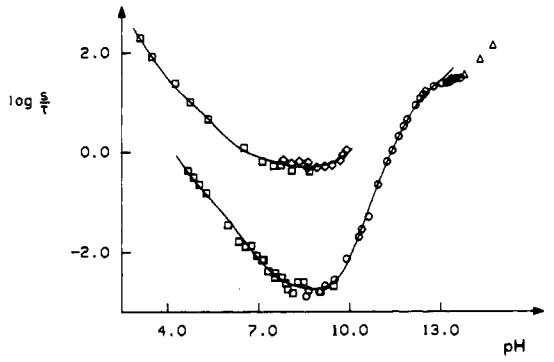

Figure 8. Logarithmic plot of the relaxation times for the ring protonation of phloroglucinol extrapolated to zero buffer concentration versus the pH of the solution: ○, stopped-flow experiments jumping from neutral to basic solutions; □, stopped-flow experiments jumping from basic to less basic solutions; ◇, pressure-jump experiments; △, temperature-jump experiments. The curves are calculated according to eqs 19 and 20.

is disturbed by the schlieren effect due to the high concentration of base.

Discussion

Due to the three hydroxy groups, three protons can dissociate from phloroglucinol. Moreover this molecule can undergo three keto–enol transformations. These reactions lead to species **1–10** in Scheme II, which furthermore includes the protonated species A (the σ-complex with pK_a = −3.2 observed by Kresge[9]) and species B. In the pH range of our investigations, A and B are intermediates of very low concentrations for the acid-catalyzed reactions of **1** to **7** and **7** to **9**, respectively; i.e., species A and B will be taken into account when reaction rates are discussed, but they will be neglected when equilibria are considered. Each column of Scheme II shows species with the same degree of dissociation, and each row contains differently dissociated species with the same degree of conjugation. All experiments reported in the previous paragraph can be explained quantitatively by this scheme.

Equilibria. Three dissociation constants are obtained from the titration curves, and eqs 5–7 connect these with the concentrations of the different species at equilibrium. K_{a1}–K_{a3} summarize over

$$K_{a1} = \frac{\{c_2 + c_6 + c_8\}c_H f_I^2}{c_1 + c_7 + c_9 + c_{10}} \quad (5)$$

$$K_{a2} = \frac{\{c_3 + c_5\}c_H f_{II}}{c_2 + c_6 + c_8} \quad (6)$$

$$K_{a3} = \frac{c_4 c_H f_I f_{III}}{\{c_3 + c_5\}f_{II}} \quad (7)$$

the concentrations of species with the same stoichiometry. Nine independent constants are needed for a complete description of

Scheme II

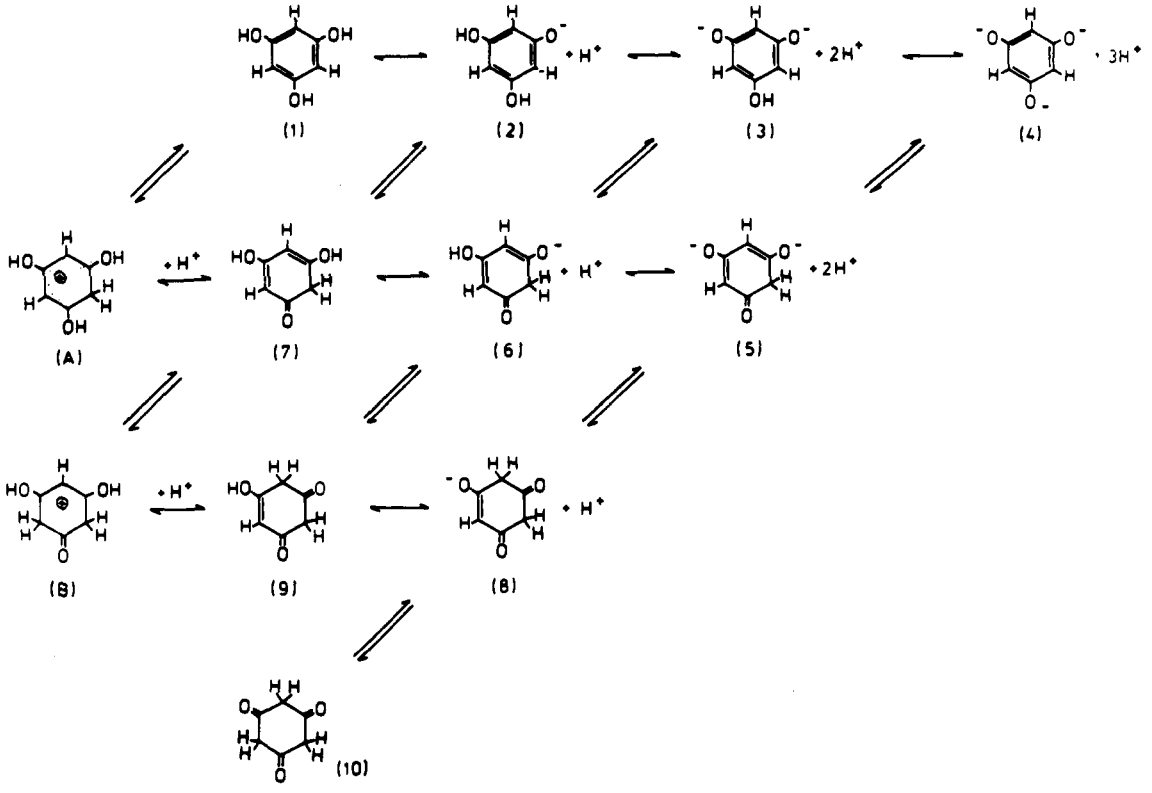

the equilibria between the ten species **1–10** in Scheme II. We choose nine dissociation constants as defined in eq 8, and all but one are obtainable from the kinetic experiments.

$$K_{ij} = \frac{c_i c_H f_i f_H}{c_j f_j} \tag{8}$$

In order to understand the meaning of the dissociation constants obtained in the stopped-flow experiments, we have to discuss the rate of the individual reaction steps. All horizontally written steps deal with the protonation of oxygen atoms. These reactions proceed with diffusion-controlled rates,[14] and they are too fast to be followed with the stopped-flow technique. On the other hand, in all diagonally written steps, the protonations are connected with keto–enol transformations, which are relatively slow[15] and occur in the time range of our equipment. (In Scheme II the rate-determining steps are indicated by two arrows ⇌, whereas the diffusion controlled steps are indicated by double arrows ⇄.) This leads to the following conclusions: (i) The very fast change in the absorbance from A_i to A_0 is caused by the protonation/deprotonation of oxygen atoms where the degree of conjugation does not change; i.e., these reactions proceed within one row of Scheme II. (ii) In the stopped-flow experiments the relaxation effects are caused by reactions involving a change in the degree of conjugation, i.e. reactions from one row to another in Scheme II. Therefore three relaxation effects can be observed at most, since Scheme II contains four rows. In the following we have to discuss the relative rate of these three reactions.

In the first set of experiments jumping from neutral to basic solutions, we start at pH = 6, where phloroglucinol exists exclusively in the aromatic form **1**,[4] and we obtain a single relaxation effect. In the second set of experiments jumping from basic solutions to less basic or acidic solutions, we start at pH = 11, where species **5** prevails,[4] and the experiments yield two relaxation effects. The relaxation time of the slow effect agrees with the corresponding value of the jump from neutral to basic in the range 8.5 < pH < 9.5, where both jumps (pH increase and pH decrease) yield relaxation effects. These results can be explained in the following way. For the jump from basic to less basic solution, species **5** equilibrates with **6** and **7**, before the fast relaxation effect starts. In the fast effect, equilibrium is established between forms **5**, **6**, and **7**, and forms **8**, **9**, and **10**, respectively, and in the slow relaxation effect, the overall equilibrium between forms **5–10** and **1–4** is reached. That means, the reaction from the first row to the second row is the slowest step. Correspondingly, at the jump from neutral to basic solution, the diffusion-controlled reactions between **1**, **2**, **3**, and **4** are at equilibrium, before the measurement starts. We observe only one relaxation effect, since the first step from the first row to the second one is rate determining and all following reactions are faster.

Finally we have to decide whether the reaction from the second row (**5**, **6**, **7**) to the third row (**8**, **9**) of Scheme II or the reaction from **8** and **9** to **10** is rate determining for the fast relaxation effect. The pH after *mixing* can be chosen such that, after the fast effect, species **7**, **9**, and **10** do not exist; i.e., equilibrium is only established between **5**, **6**, and **8**. Also in this case the fast relaxation effect is observed, which shows that the reaction from the second row to the third row of the scheme causes the fast relaxation effect. On the other hand we can jump to pH < 4, where after the fast effect the equilibrium is shifted completely to the uncharged species (**7**, **9**, and **10**). Under these conditions the spectrum shows no absorption for λ > 220 nm. This indicates that the triketone **10** predominates, because the dienone **7** and the enone **9** should absorb strongly (see Figure 6), whereas the weak absorbance of the unconjugated carbonyl groups cannot be observed at the low concentrations used. Thus species **10** is obtained as an intermediate in the reaction, and the step from the second to the third row is slower than the reaction from the third row to species **10**. The result of these considerations is that reactions 9 and 10 cause the slow and the fast relaxation effects, respectively, and that reaction 11 is faster than reaction 10 and cannot be observed. In eqs 9–11 species separated by commas are in fast preequilibria.

$$\{1, 2, 3, 4\} \rightleftharpoons \{5, 6, 7, 8, 9, 10\} \tag{9}$$

$$\{5, 6, 7\} \rightleftharpoons \{8, 9, 10\} \tag{10}$$

$$\{8, 9\} \rightleftharpoons \{10\} \tag{11}$$

(14) Eigen, M. *Angew. Chem.* **1963**, *75*, 489–508.
(15) (a) Bednar, R. A.; Jencks, W. P. *J. Am. Chem. Soc.* **1985**, *107*, 7117–7126. (b) Lin, A. C.; Chiang, Y.; Dahlberg, D. B.; Kresge, A. J. *J. Am. Chem. Soc.* **1983**, *105*, 5380–5386. (c) Bernasconi, C. F. *Pure Appl. Chem.* **1982**, *54*, 2335–2348.

Now we can appoint reactions to the pK values obtained in the stopped-flow experiments. For the jump from neutral to basic solutions, equilibrium is established within the first row of Scheme II during the very fast absorbance change from A_i to A_0. Correspondingly, immediately after mixing, the spectra show the absorption of aromatic compounds without any indication of the existence of conjugated ketones. A_0 can be measured with sufficient accuracy only in the range pH < 12.5, and therefore species **4** has not to be considered. The pH dependence of A_0 fits to a single deprotonation (see Figure 2); i.e., the pK_α value corresponds to the step from **1** to **2**. The second dissociation to **3** cannot be observed, since the spectra of **2** and **3** are very similar and $K_{21} \gg K_{32}$ (see below). Therefore K_α is defined by eq 12. In the following slow relaxation, the overall equilibrium is reached and the final absorbance A_e is determined by eqs 5 and 6.

$$K_\alpha = \frac{c_2 c_H f_1^2}{c_1} \tag{12}$$

For pH jumps from pH = 11 to lower values, we start from species **5**, and at $t = 0$ the equilibrium is established between **5**, **6**, and **7**. The two dissociation constants obtained from A_0 (see Figure 3) are therefore defined by eqs 13 and 14. The optical

$$K_{\beta 1} = \frac{c_5 c_H f_{II}}{c_6} \tag{13}$$

$$K_{\beta 2} = \frac{c_6 c_H f_1^2}{c_7} \tag{14}$$

spectra of species **6** (y in Figure 5a) and **7** (z in Figure 5a) are recorded at $t = 0$, where equilibrium is estabished between **5**, **6**, and **7** but the other species do not yet exist. They are similar to the spectrum of the dianion of filicinic acid (z in Figure 6), indicating the dienonic structure of **6** and **7**. During the fast relaxation effect **5**, **6**, and **7** equilibrate with **8**, **9**, and **10**. Correspondingly, the two dissociation constants obtained from A_1 (see Figure 4) are described by eqs 15 and 16. The spectrum of **8**

$$K_{\gamma 1} = \frac{c_5 c_H f_{II}}{c_6 + c_8} \tag{15}$$

$$K_{\gamma 2} = \frac{(c_6 + c_8) c_H f_1^2}{c_7 + c_9 + c_{10}} \tag{16}$$

is recorded at pH = 7 and $t = t_1$ (y in Figure 5b). It shows a single absorption band at $\lambda = 278$ nm, which is typical for cyclic enones such as dimedone (x, y in Figure 6). At pH < 4 and $t = t_1$ the spectrum shows no absorption for $\lambda > 220$ nm. Therefore under these conditions the triketone **10** prevails over the enones **7** and **9**. Again the pH dependence of the final value A_e yields no new information.

Thus the measurements yield eight independent equilibrium constants defined by eqs 5–7 and 12–16. These constants allow us to calculate all individual equilibria in Scheme II except of that between species **9** and **10**, for which only a limiting value can be estimated from the relation $c_9 \ll c_{10}$. However, the accuracy of the measurements is not sufficient to obtain precise values for all of these equilibrium constants. Therefore we evaluate the amplitudes of pressure-jump experiments for further information. These measurements are performed in the range 7.8 < pH < 10.1, where at equilibrium only species **1**, **2**, **5**, and **8** have to be considered according to the results of the stopped-flow experiments. In this range we observe two relaxation effects, but only the faster one, which is due to the reaction between **5** and **8**, is evaluated. (The reaction from forms **5** and **8** to forms **1** and **2** causes the slow relaxation effect.) The solutions are buffered with $NH_4Cl/NaOH$, and the relaxation is observed at $\lambda = 350$ nm, where only species **5** absorbs light. The relaxation amplitude is given by eqs 17 and 18, where c_0 is the total concentration of phloroglucinol and the dissociation constants are defined in eq 8. Fitting these equations to the experimental results (Figure 7) yields $K_{28}/K_{21} = 10^{8.9}$ mol dm^{-3} ± 25% and $K_{58} = 10^{-8.8}$ ± 20%.

$$\delta A^{350} = \epsilon_5^{350} d \frac{\Gamma \Delta V^\circ \delta p}{RT} \tag{17}$$

$$\Gamma = c_0 \left(2 + K_{28} + \frac{K_{58}}{c_H f_{II}} + c_H \left(\frac{f_1^2 K_{28}}{K_{21}} + \frac{f_{II}}{K_{58}}(1 + K_{28}) \right) + c_H^2 \frac{f_1^2 f_{II} K_{28}}{K_{58} K_{21}} \right)^{-1} \tag{18}$$

The results of all measurements yield eight of the nine dissociation constants defined by eq 8. They are summarized in Table I. All curves in Figures 1, 2, 3, 5, and 7 are calculated with these constants.

Kinetics. So far the relaxation amplitudes have been evaluated, and now the relaxation times will be discussed. Using the stopped-flow technique, we can follow only the two reactions 9 and 10. In order to derive the rate equations for these reactions, we have to consider two different ways for each deprotonation of phloroglucinol to occur: (i) the loss of a proton and (ii) the reaction of the phloroglucinol with a hydroxyl ion with the release of a water molecule. Correspondingly, for each step from "j" to "k" we need two rate constants k_{jk} for the proton transfer (i) and k_{jk}' for the reaction with hydroxyl ions (ii). The integration yields eq 2 corresponding to first-order kinetics, since the solutions are buffered, i.e. c_H = constant. For the integration we take into account that the two relaxation times differ at least by a factor of 10 (kinetically decoupled reactions), and we consider all preequilibria. Thus we obtain the rather complicated eqs 19 and 20 for the relaxation times. The derivation of these equations is given in ref 13, where activity corrections have been discussed also.

$$1/\tau_F = \frac{k_{58} c_H + k_{58}' + k_{69} K_{56}^{-1} c_H^2 + k_{69}' K_{56}^{-1} c_H}{1 + K_{56}^{-1} c_H + (K_{56} K_{67})^{-1} c_H^2} + \frac{k_{7B} (K_{56} K_{67})^{-1} c_H^3}{1 + K_{56}^{-1} c_H + (K_{56} K_{67})^{-1} c_H^2} + \frac{k_{85} + k_{85}' K_W c_H^{-1} + k_{96} K_{89}^{-1} c_H + k_{96}' K_W K_{89}^{-1}}{1 + K_{89}^{-1} c_H + K_{810}^{-1} c_H + (K_{89} K_{9B})^{-1} c_H^2} + \frac{k_{B7} (K_{89} K_{9B})^{-1} c_H^2}{1 + K_{89}^{-1} c_H + K_{810}^{-1} c_H + (K_{89} K_{9B})^{-1} c_H^2} \tag{19}$$

For the numerical evaluation of the slow relaxation effect, the values of all equilibrium constants are inserted into eq 20, and the five rate constants listed in Table I are obtained. In Figure 8 the solid line for $1/\tau_S$ is calculated with these constants. Likewise eq 19 can be fitted to the values measured for the fast relaxation time. However, this procedure yields no unambiguous values for the rate constants involved in the fast reaction. The curve for $1/\tau_F$ is calculated with one consistent set of constants. For pH > 13 the calculated curve of $1/\tau_S$ differs significantly from the experimental data. This is due to the fact that the activity corrections cannot be performed satisfactorily at high ionic strength. Details of the numerical evaluation (including activity corrections) are described in ref 13.

$$1/\tau_S = \frac{k_{54}' K_W}{c_H N_2} + \frac{k_{45}' K_{43}}{c_H N_1} + \frac{k_{54}}{N_2} + \frac{k_{45} K_{43}}{N_1} + \frac{k_{63}' K_W}{K_{56} N_2} + \frac{k_{36}'}{N_1} + \frac{k_{63} c_H}{K_{56} N_2} + \frac{k_{36} c_H}{N_1} + \frac{k_{72}' K_W c_H}{K_{56} K_{67} N_2} + \frac{k_{27}' c_H}{K_{32} N_1} + \frac{k_{72} c_H^2}{K_{56} K_{67} N_2} + \frac{k_{27} c_H^2}{K_{32} N_1} + \frac{k_{A1} c_H^3}{K_{56} K_{67} K_{7A} N_2} + \frac{k_{1A} c_H^3}{K_{21} K_{32} N_1} \tag{20}$$

with

$$N_1 = 1 + \frac{K_{43}}{c_H} + \frac{c_H}{K_{32}} + \frac{c_H^2}{K_{21} K_{32}} \tag{21}$$

and

$$N_2 = 1 + (K_{56}^{-1} + K_{58}^{-1}) c_H + ((K_{56} K_{67})^{-1} + (K_{89} K_{58})^{-1} + (K_{810} K_{58})^{-1}) c_H^2 + (K_{56} K_{67} K_{7A})^{-1} c_H^3 \tag{22}$$

Table I. pK Values and Rate Constants Obtained by Evaluating Relaxation Amplitudes and Relaxation Times[a]

$pK_{21} = 8.90 \pm 0.05$	$pK_{58} = 8.71 \pm 0.1$
$pK_{32} = 9.9 \pm 0.3$	$pK_{67} = 5.14 \pm 0.05$
$pK_{43} = 12.75 \pm 0.05$	$pK_{89} < 4.7$
$pK_{45} = 14.10 \pm 0.15$	$pK_{810} = 5.7 \pm 0.2$
$pK_{56} = 7.43 \pm 0.05$	
$k_{1A} = 11 \pm 3$ dm^3 mol^{-1} s^{-1}	$k_{36}' = (2.1 \pm 0.9) \times 10^{-2}$ s^{-1}
$k_{27} = (6.4 \pm 4.0) \times 10^4$ dm^3 mol^{-1} s^{-1}	$k_{45}' = 21.9 \pm 1.1$ s^{-1}
$k_{27}' = (2.5 \pm 1.8) \times 10^{-3}$ s^{-1}	

[a] The dissociation constants and the rate constants are defined by eqs 8 and 20, respectively; $T = 20$ °C.

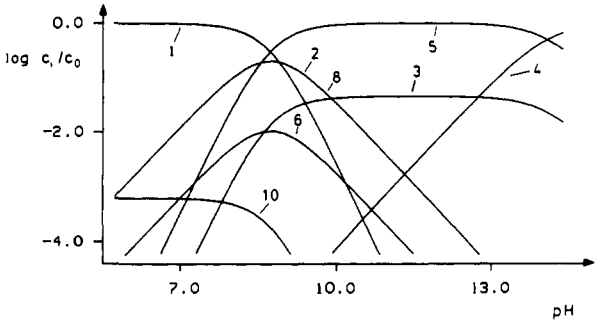

Figure 9. Logarithmic plot of the relative concentrations of the different species of phloroglucinol versus the pH of the solution. The concentrations of **2** and **8** are equal, and the concentrations of **7** and **9** are too small to be registered.

General Conclusions. For the first time, all dissociation and keto–enol equilibria of phloroglucinol are determined: they can be calculated from the pK values summarized in Table I. At equilibrium the uncharged molecule exists predominantly in the aromatic form **1**, whereas the concentrations of the aromatic anion **2** and the enonic anion **8** are approximately equal, and the dianion prevails as dienone **5**. For the trianion only the aromatic form **4** is feasible. All other species except **9** are observed as intermediates. The spectra of **1**–**4** indicate the aromatic structure. The spectra of **5**, **6**, and **7** (Figure 5a) and **8** (y in Figure 5b) are reported. The triketone **10** shows no absorption in the range $\lambda > 220$ nm. The spectra indicate unambiguously the degree of conjugation. At a constant degree of conjugation the absorption bands increase and are shifted to longer wavelengths with the degree of dissociation.

The keto–enol equilibrium increases strongly with the degree of dissociation; i.e., the formation of the ketone is favored by the increasing charge density of the aromatic ring. For phloroglucinol itself we have $c_7/c_1 = 1/10^5$, for the anion $c_6/c_2 = 1/20$, and for the dianion $c_5/c_3 = 20$. Within the range of the ketonic structures, those are preferred which have the lowest degree of conjugation, i.e. $c_{10} \gg c_9 + c_7$ and $c_8 \gg c_6$. The existence of the triketone has been postulated already in 1886, and from the data of Table I, we calculate $c_{10}/c_1 = 6 \times 10^{-4} \pm 50\%$. These considerations are summarized in Figure 9.

The kinetic results show that the rate of ring-protonation increases with decreasing degree of conjugation, as is generally observed.[15] Our value for k_{1A} agrees well with $k_{1A} = 38$ dm^3 mol^{-1} s^{-1} obtained at 33 °C by Kresge et al.[16] The protonation of the aromatic ring is connected with the formation of a σ-complex, and for many compounds the rate constants of this reaction have been measured.[7,17] These constants refer to the direct protonation of the aromatic ring, whereas two of our rate constants refer to the reactions of the ring with a water molecule with the abstraction of a hydroxyl ion. In order to be able to correlate our data to those given in the literature, we have to estimate the corresponding rate constants for the direct proton transfer in the following way. In a Brönsted plot, the logarithm of the rate constant of a protonation versus the pK_a of the proton donor yields a straight line with a slope close to 0.5; e.g., for the protonation of the aromatic ring of 1,3,5-tripyrrolidinobenzene, the slope is 0.44.[17a] Within experimental error, this slope agrees with the difference log k_{27} – log k_{27}' of phloroglucinol (using p$K_a = 15.7$ for water and p$K_a = -1.7$ for H_3O^+). We use the same value for the protonation of the aromatic anions **3** and **4** and obtain $k_{45} = 10^9$ dm^3 mol^{-1} s^{-1} and $k_{36} = 10^6$ dm^3 mol^{-1} s^{-1} from the values of k_{45}' and k_{36}'. Thus all rate constants are known for the reaction of the aromatic species **1**, **2**, **3**, and **4** to the dienones A, **7**, **6**, and **5**, respectively. These are compared to the rate constants for other σ-complex formations by a Brönsted plot in Figure 10, where log (k/q) is plotted versus the pK_a of the complex. The statistical factor q is the number of equivalent positions for the protonation. The values for phloroglucinol fit well to the data from the literature, indicating that all σ-complex formations proceed according to the same mechanism.

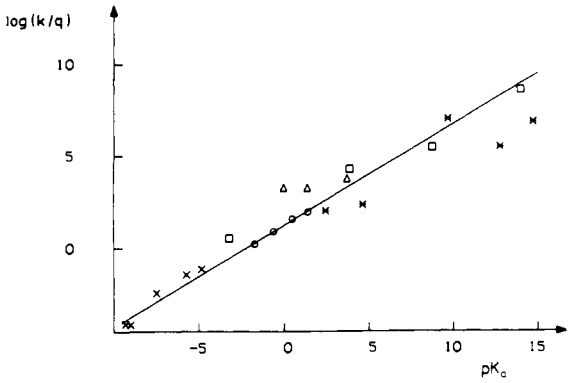

Figure 10. log (k/q) versus the pK_a value for the protonation of aromatic compounds: ×, substituted benzenes; O, azulenes; Δ, substituted pyrroles; ✱, triaminobenzenes; □, phloroglucinol.

Acknowledgment. The authors are indebted to the Fonds der Chemischen Industrie for financial support of this work and for a scholarship (Doktorandenstipendium) to M.L.

Supplementary Material Available: Derivations of eqs 17–22 (7 pages). Ordering information is given on any current masthead page.

(16) Kresge, A. J.; Chiang, Y.; Shapira, S. A. *Can. J. Chem.* **197**, *49*, 2777–2784.

(17) (a) Sachs, W.; Knoche, W.; Herrmann, Ch. *J. Chem. Soc., Perkin Trans. 2* **1991**, 701–712. (b) Kresge, A. J.; Mylonakis, S. G.; Sato, Y.; Vitullo, V. P. *J. Am. Chem. Soc.* **1971**, *93*, 6181–6188.